inter.noise 2014
MELBOURNE AUSTRALIA
16-19 NOVEMBER

Experimental and numerical tools for the characterization of ultrasonic propagation for nuclear reactor application

Nicolas VAN DE WYER[1]; Christophe SCHRAM[1]; Dries VAN DYCK[2]; Marc DIERCKX[2]

[1] von Karman Institute for Fluids Dynamics, Belgium

[2] Belgian Nuclear Research Center, Belgium

ABSTRACT

Due to being cooled by liquid metal, the next generation of nuclear reactors requires an ultrasonic visualization system for internal inspection and object detection. In such environment, acoustic propagation is submitted to peculiar conditions in terms of temperature and velocity gradients. In the core of the nuclear reactor, temperature gradients are 5K over 0.1 m and the velocity gradients reach 1 m/s over 0.2 m. The effects of these conditions on the ultrasonic propagation are investigated in a specific water facility, reproducing conditions similar to the nuclear application. The design and the characteristics of this new facility are presented in this paper. This includes a shadowgraph system for the visualization of the propagation of the acoustic wave in various conditions. The acoustic similitude between water and liquid metal is discussed for ensuring the validity of the water test for nuclear application. The propagation of ultrasonic waves in the full scale application is modeled by using a ray tracing algorithm. The validation of this algorithm has been performed by comparing the results with data from literature and numerical acoustic calculation. Preliminary results obtained with this algorithm are shown in the paper.

Keywords: Underwater acoustic, ultrasounds I-INCE Classification of Subjects Number(s): 21.8.2 and 73.5
(See http://www.inceusa.org/links/Subj%20Class%20-%20Formatted.pdf.)

1. INTRODUCTION

The MYRRHA project (for **Multi-purpose hYbrid Research Reactor for High-tech Applications**) concerns the development of a multi-purpose flexible irradiation facility. This generation IV reactor is conceived as an Accelerator Driven System (ADS), able to operate in sub-critical and critical modes and cooled by Lead-Bismuth Eutectic (LBE). The aims of this project is demonstrating the feasibility of the ADS technology and the cooling concept for fast-neutron reactor (1).

In a nuclear reactor, the coolant liquid is used for extracting the heat produced by the nuclear reaction from the core of the reactor, and, in most of the case, transporting this heat to the energy production unit. This allows maintaining the core of the reactor in an acceptable range of temperature. In most nuclear power plants, the coolant is light purified water under high pressure for avoiding boiling. Furthermore, the water is a neutron moderator and cannot be used in fast-neutron reactor. In this type of reactor, lead-bismuth is a good alternative to the water. Indeed, the neutrons are less slowed by interaction with heavy nuclei. The boiling temperature of the lead-bismuth under ambient pressure (2023 K) is high enough over the reactor core temperature (923 K) for avoiding the risk of significant pressurization of the reactor by overheating.

If the lead-bismuth eutectic is an efficient and safe coolant for fast-neutron reactor, the opacity of this liquid metal is problematic for the required inspection and maintenance processes of the reactor core. This opacity makes the conventional optical method impossible. For solving this inspection issue, an imaging technique based on the propagation of ultrasounds is used (2). The ultrasonic imaging technique is intensively used for other applications, like the echography in the medical field, the sonar for naval application or for non-destructive material inspection. The technique is based on the determination of traveling time of an ultrasonic pulse in the medium. This time is defined as the time elapsed between the emission of a pulse and the reception of the reflexion of this pulse due to impedance mismatch at the surface of an inhomogeneity in the medium. The determination of the pulse in the time signal is

[1] vandewyer@vki.ac.be

based on the envelope of the signal determined via the Hilbert transform (3). From the position of the ultrasonic sensor and the sound velocity in the medium, the exact position of the surface is calculated. By repeating this operation at various positions in a region, the 3D shape of the surfaces of this region can be reconstructed.

The use of ultrasonic imaging techniques for application in a nuclear environment under liquid metal requires some new development effort due to the specific conditions of this environment. These conditions include high temperature (450 K - 720 K), chemical activity of liquid metal, strong gamma radiation (up to 30 kGy/h) and velocity and temperature gradients. A high temperature ultrasonic sensor capable to cope with the radiation levels present in the MYRRHA reactor has been developed by the Belgian Nuclear Research Centre (SCK-CEN) and the Kaunas University of Technology (Lithuania) (4) (5). The sensors demonstrated a good long time performance in a liquid lead-bismuth alloy. Their pulse response was also shown to be suitable for visualization purposes. A number of other issues have been addressed as well, described in a comprehensive review by E. Jasiuniene (6). The conclusions of that review indicated that no optimum imaging techniques had been clearly demonstrated for nuclear applications. Nevertheless, it was emphasized that given the harsh conditions in which the ultrasonic system has to operate, it is better to keep the system configuration as simple as possible.

The aim of the TAUPE (Technologies for the Amelioration of Ultrasonic imaging in a Pool of lead-bismuth Eutectic) project is to develop an imaging technique for the structure inspection and object detection and also to investigate numerically and experimentally the effect of temperature gradient and velocity gradient on the ultrasonic wave propagation. This project, supervised by the SCK-CEN, is carried out at the von Karman Institute (VKI).

2. THE TAUPE FACILITY

The TAUPE project considers the development and the experimental characterization of an ultrasonic imaging technique for the MYRRHA application. This includes the effect of the presence of temperature and velocity gradient in the core of the reactor. Furthermore, it was decided to use the Shadowgraph technique for visualizing the ultrasonic beam propagation. The requirements for the experimental facilities of the TAUPE project are then: 1) allowing the validation of the detection algorithm over realistic dimensions, 2) obtaining controlled velocity and temperature gradients, and 3) permitting the visualization of an ultrasonic beam by the Shadowgraph technique.

2.1 The experimental medium

The acoustic characteristics of lead-bismuth at 570 K and of the water at 293 K are similar in terms of sound velocity (respectively about 1500 and 1750 m/s), and therefore also in beam shape, wavelength and resolution. Furthermore, the signal-to-noise ratio in water was shown higher than in lead-bismuth. This is due to to a better matching of the impedance of the LBE with the piezo and stainless steel lens of the sensor. Furthermore, the acoustic absorption in lead-bismuth is much less as in water. All these points make the investigation of the propagation of ultrasound waves in water conservative for application in lead-bismuth (7). It was thus decided to perform all experimental tests in water. This allows avoiding the use of expensive and toxic lead-bismuth, and using the Shadowgraph technique for the visualization of the propagation of ultrasound waves.

2.2 Ultrasonic sensor characterization

A description of an ultrasonic sensor usable in the core of a nuclear reactor has been investigated by Kazys in 2007 (4). In the case of the TAUPE project, the experimental conditions are clearly less peculiar and a regular immersed circular sensor A309S-SU from Olympus is used. The optimal pulse frequency of the sensor is chosen for having the lowest acoustic pressure attenuation considering the distance range in MYRRHA. This attenuation is due to the geometrical beam spreading and the acoustic absorption principally. These attenuation are given respectively by the relations (8):

$$\frac{p}{p_0} = \frac{D_t^2 . f}{c.L} \qquad \frac{p}{p_0} = e^{-\alpha_p . L} \tag{1}$$

where p and p_0 are respectively the local and the initial pressure amplitude, D_t is the diameter of the sensor, f is the frequency of the pulse, c is the sound velocity, L is the propagation distance, and α_p is the acoustic absorption coefficient. Considering that this coefficient is given as a function of the square of the pulse frequency, the acoustic pressure attenuation due to the two phenomena is given by combining the

two relations:

$$\frac{p}{p_0} = \frac{D_i^2.f}{c.L}.e^{-K_\alpha.f^2.L} \quad (2)$$

The contributions of the two phenomena having an opposite behavior as a function of the frequency, an optimal pulse frequency can be determined from the relation 2. Considering two distance ranges for the MYRRHA application, 0.05-0.3 m and 2-3m, a pulse frequency of 5 MHz is a good balance between the two optimum frequencies corresponding to the two distance ranges (15 and 3.2 MHz respectively).

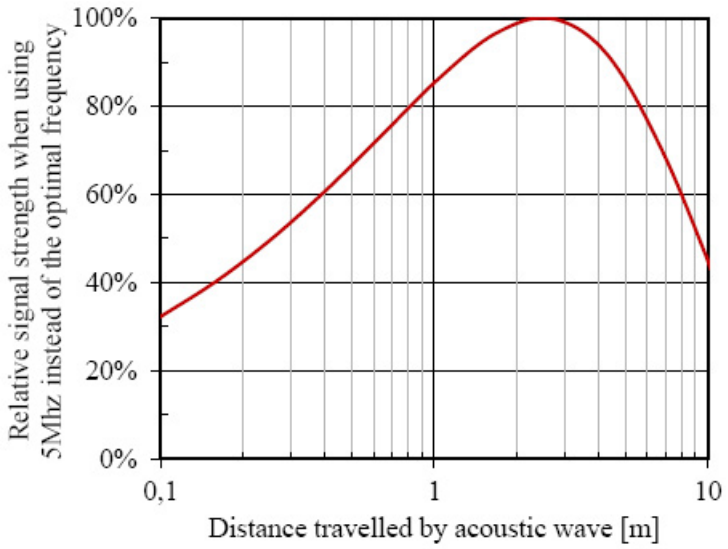

Figure 1 – Extra pressure loss induced by the use of 5 MHz sensor instead of optimal 3.2 MHz sensor.

The extra pressure loss due to the use of a 5 MHz sensor instead of an optimal 3.2 MHz is presented on Fig.1. This extra loss is derived from the relation 2 and shows a maximum of 25%. This value is acceptable for the considered application.

2.3 The geometry of the facility

Concerning the dimension of the facility, the first and the third requirements for the experimental facility are incompatible. On the one hand, the respect of the dimensions representative of the real configuration induces the use of a pool of 2000 mm length and width, 2500 mm deep. On the other hand, the quality of the images from the Shadowgraph technique is decreasing with the distance traveled by the light beam in the water. The width of the facility should thus be minimized in order to preserve the Shadowgraph image quality. It was finally decided to use two facilities for the experimental validation of the detection algorithm in order to respect the various requirements of the investigation. The first facility is dedicated to the validation of the detection algorithm alone over an area representative of the MYRRHA reactor, without taking into account the particular conditions of the nuclear environment. In the second facility, the effect of the long distances traveled, and of the temperature and velocity gradients are investigated. This second facility is specially designed for the visualization of the propagation of the ultrasound waves by Shadowgraph.

The facility used for the experimental validation of the detection algorithm is a 2000 mm x 2000 mm water pool with a depth of 250 mm equipped with a 2D displacement system for moving the ultrasonic sensor over the entire surface of the pool.

The second facility is dedicated to the investigation of the effects of the MYRRHA environment on the propagation of ultrasounds. The depth of the facility is 2500 mm, representative of the depth of the MYRRHA reactor. The width of the facility is determined by the balance between the quality of the images from the Shadowgraph system and the minimization of the influence of the walls on the measurements. The quality of the images from the Shadowgraph is decreasing with the width of the water traveled by the optical beam. The facility has thus to be as thin as possible for high quality images. But at the same time, the propagation conditions are supposed to be representative of the conditions in the MYRRHA reactor, meaning in free flow. The facility has thus to be large enough to avoid interaction of walls on the acoustic waves propagation. After preliminary tests conducted with a small water tank, it was found that a width of 300 mm should allow avoiding this interaction and giving sufficient quality for the visualization. The length of the facility has been determined from CFD calculations in order to obtain a well-controlled

velocity gradient. This system, which is described here after, requires a minimum length of 1500 mm. The final dimension of the facility is 300 x 1500 x 2500 mm. A 3D view of the facility is presented on the left hand side of Fig.2.

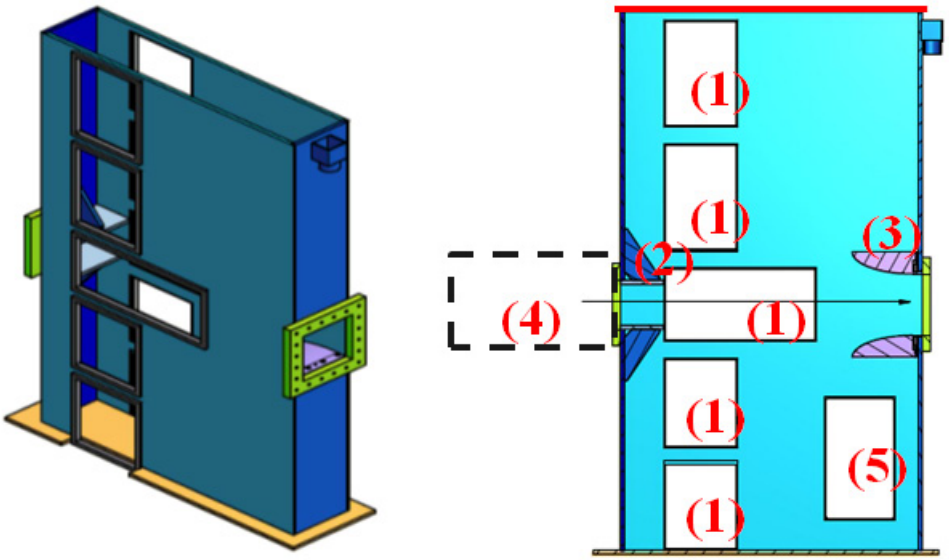

Figure 2 – 3D view (left) and detailed view of the second TAUPE facility with optical accesses (1), inlet and outlet for the circulation circuit (2) (3), velocity gradient generator (4), and technical access (5).

The Shadowgraph system, based on the passage of a light beam in the test section, requires optical accesses. These accesses, located on the two large sides of the pool, cover the entire height of the pool. This configuration allows visualizing the ultrasound propagation over 5 meters with a reflection on the ground surface at mid-distance. The width of the optical accesses is 370 mm in order to cover the deviation of the acoustical beam due to the velocity and temperature gradients, as well as the beam divergence over large distances. At mid-height of the pool, the optical accesses are larger with a width of 750 mm. This position in the pool corresponds to the localization of the velocity gradient generator. The large optical accesses allow the investigation of the effects of various velocity gradients, and for various incident angles of the acoustic wave. The detailed view of the facility is presented on the right hand side of Fig.2 with the various technical elements.

The cooling of the core of the MYRRHA reactor requires the circulation of the lead-bismuth between the core and the heat-exchangers. This circulation introduces velocity gradients in the vessel. Numerical simulations have shown that these gradients have a magnitude of 1 m/s over 200 mm. The presence of these gradients influences the propagation of the ultrasound waves used for the detection of the objects. As this influence needs to be quantified, the second facility of the TAUPE project will be equipped with a velocity gradient generator providing a gradient equal in magnitude to the gradient determined numerically.

The cooling system of the MYRRHA reactor induces the circulation of a cold flow from the heat exchangers and the core in the vessel of the reactor. This flow creates a temperature gradient with the free region around. Furthermore, the fuel assemblies generate a substantial amount of heat, inducing also temperature gradients. The presence of temperature gradients in the vessel of the MYRRHA reactor is another element that influences the propagation of the ultrasound waves of the detection system. This influence has also to be characterized experimentally in order to be taken into account in the detection program. The second facility of the TAUPE project will be equipped with a temperature gradient generator reproducing the temperature gradient of 5 K over 0.1 m created by the fuel assemblies.

2.4 The Shadowgraph system

This second facility is equipped with a Shadowgraph system for the visualization of the propagation of the ultrasonic waves in the water. The feasibility of the visualization of ultrasonic wave's propagation in water by means of the Shadowgraph technique has been reported in the literature since long time (9). This technique is based on a system of parallel light beams, traveling through a homogeneous medium. The light beams are generated by a punctual light source and are collimated through a lens or parabolic mirror. After the passage in the test medium, the light beams are converged through a second lens or

parabolic mirror. The image is then recorded by a high speed camera. The ultrasonic waves traversing the test medium create a local variation of the refractive index, inducing a local deviation of the light beam (10). This deviation creates dark and light regions in the image corresponding to the waves. The optical technique allows the visualization of numerous acoustic phenomena with high spatial and temporal resolution (11). For compactness reasons, the Shadowgraph system mounted on the TAUPE facility is composed of two parabolic mirrors and two flat mirrors. The two parabolic mirrors collimate the light beam from the light source and to the camera. The two flat mirrors allow locating the parabolic mirrors along the facility perpendicularly to the large sides, and thus decreasing the dimensions of the installation. The parallel light beam traveling parallel to the facility will be reoriented through the optical accesses via the flat mirrors. All the elements of the Shadowgraph system, composed by the mirrors, light source, lens and camera, are mounted on a single structure. This structure is moved by four vertical displacement systems in order to cover the entire height of the pool with the visualization system. The use of a single structure supporting all the elements of the Shadowgraph allows avoiding misalignment of these elements during the motion of the system. The Shadowgraph used in this project is composed of two parabolic mirrors and two flat mirrors of respectively 300 and 400 mm diameter, a car lamp as light source, a high speed camera with a maximum acquisition frequency of 6 kHz, and a small lens for focusing the light beam. The structure supporting the Shadowgraph system is independent on the pool. This allows avoiding the transmission of the vibrations from the different systems mounted on the pool (principally the velocity gradient generator) to the elements of the Shadowgraph. Furthermore, all the elements of the different structures and water pump are mounted on anti-vibrating systems. The Shadowgraph system is presented on Fig. 3 with the pool and the displacement systems. The U-shape structure supporting all the Shadowgraph elements (dark grey), is fixed on four vertical carriages (blue column) independent of the pool.

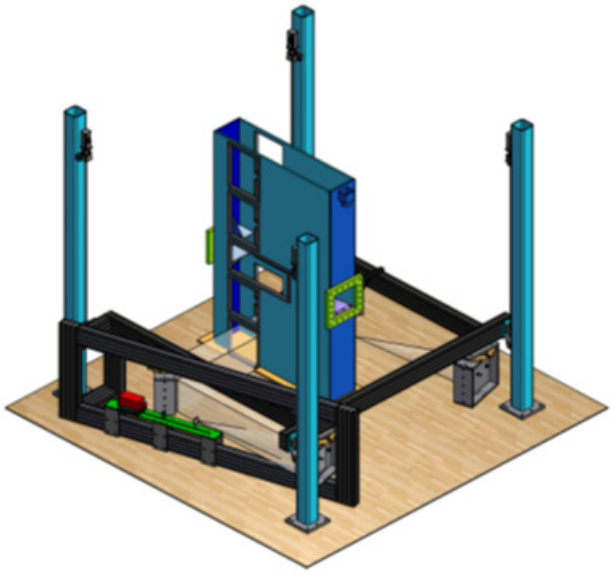

Figure 3 – Second TAUPE facility with the Shadowgraph system (dark grey) fixed on four vertical displacement systems (vertical blue columns).

3. THE MODELING OF ULTRASOUND PROPAGATION

Various methods for the modeling of the propagation of an ultrasonic pulse exist and have advantages and disadvantages. The finite element method (FEM) and boundary element method (BEM) are based on the discretization of the region considered in volumic or surfacic elements, respectively. The wave equations are then solved by means of numerical methods. A limitation of these approaches stands in the large computational cost involved in the resolution of ultrasonic waves. Indeed, as a rule of thumb, a minimum of 6 to 10 elements per wavelength are required to minimize dispersion errors, 15 elements per wavelength being considered as more conservative for the application at stake. In the case of an ultrasonic wave at 5 MHz, this means elements of 0.02 mm. In the case of a 2D calculation over a region of 300 x 300 mm, the mesh is composed of 225 million of points, requiring enormous computational resources, practically unavailable with conventional clusters. The modeling of the propagation of ultrasonic

waves over the real dimension of the second TAUPE facility with a FEM or BEM approach is thus not affordable. Another method for the modeling of acoustic propagation is based on an alternative approach based on geometrical acoustics: the ray-tracing method. The principle of this method is to consider the decomposition of an acoustic wave front in a set of rays. It is based on the high frequency approximation, meaning that the characteristic dimensions of the propagation domain are large compared to the wave length. In this method, the direction and velocity of propagation of each ray is depending on the local conditions only.

3.1 The ray-tracing method

The propagation of the rays representing the acoustic wave front is calculated from the eikonal equation and the definition of the unit vector perpendicular to the front $\bar{v}$ (12). The eikonal equation is derived from the development of the fluctuation of the pressure from the mass and momentum conservation equations and in series of inverse power of the frequency. This development gives an equation of second order on the frequency. By considering the equation valid for all frequencies, each term of the equation has to be zero. The second order term gives the eikonal equation that can be rewritten by using the wave vector k:

$$|k(x)|^2 = \frac{\omega^2}{c(x)^2} \tag{3}$$

The trajectory of a ray is given by:

$$dX = c.\bar{v}dt \qquad \Rightarrow \qquad \frac{dx_i}{dt} = c.\frac{k_i}{|k|} \tag{4}$$

where X is the position of the ray at time t, x_i and k_i represent respectively the components of X and k. The variation of the direction of the propagation is given by:

$$\frac{dk_i}{dt} = \frac{\delta k_i}{\delta x_j}.\frac{dx_j}{dt} = c.\frac{\delta k_i}{\delta x_j}.\frac{k_j}{|k|} \tag{5}$$

By considering $rot(\bar{k}) = 0$:

$$\frac{\delta k_i}{\delta x_j} = \frac{\delta k_j}{\delta x_i} \qquad \Rightarrow \qquad \frac{dk_i}{dt} = -k.\frac{\delta c}{\delta x_i} \tag{6}$$

In the previous relations, the sound velocity is the local sound velocity depending on the local temperature of the medium.

In case of medium motion, the propagation of the acoustic wave front is depending also on the wave convection, and the variation of the direction of propagation has to take into account the refraction of the wave by the velocity gradient. These two elements are considered by the ray tracing method by using the following relations:

$$dX = c.\frac{k_i}{|k|} + V_i \tag{7}$$

$$\frac{dk_i}{dt} = -k.\frac{\delta c}{\delta x_i} - k_j.\frac{\delta V_j}{\delta x_i} \tag{8}$$

Equations 7 and 8 are solved following a time-stepping procedure based on the initial position and propagation direction of each ray. The time step used in the calculation has to be a compromise between the computational time and the flow characteristic scale. This scale is depending on the length of the variation of the medium characteristics. The resolution of the equations is based on a fourth order Runge-Kutta method.

The reflection of acoustic rays on a surface is taken into account by determining the normal to the surface at the impact point and applying the reflection-law for optical ray. This method implies that only specular reflection is considered.

3.2 Validation of the ray-tracing code

The ray-tracing method presented above has been implemented and validated by comparison with various other methods for different configurations. The first validation case consider an acoustic source placed in a Bickley's profile jet (13). The jet is centered in $y = 0$, have a half width of 0.1 m and a Mach number of 0.5. The acoustic source is located in the center of the jet. This configuration has been

calculated by the means of the COOLFluiD CFD code and of the ray-tracing algorithm. Figure 4 presents the velocity field corresponding to the Bickley's profile jet considered on the left hand side. The acoustic fields induced by the source calculated via COOLFluiD is presented as the color background on the right hand side of Fig.4. The acoustic wave fronts calculated via the ray-tracing code have been superposed on this background as red stars. The similitude of the wave fronts from the two calculation methods validates the ray-tracing code.

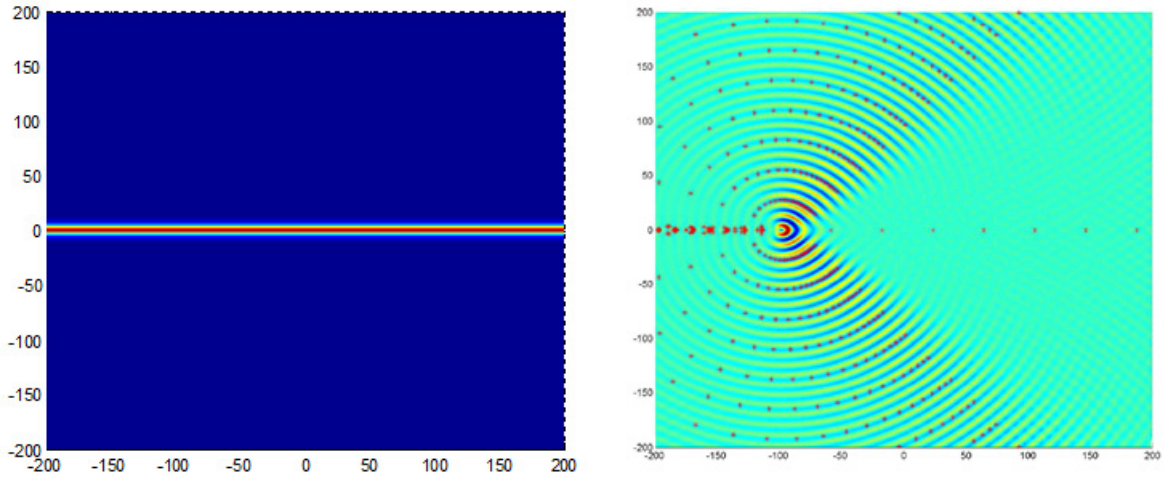

Figure 4 – Velocity profile (left) and acoustic field (right) created by an acoustic source located in the center of a Bickley's profile jet from COOLFluiD (background) and from a ray-tracing code (red points).

A second validation case is based on the deviation of acoustic waves in an ocean due to the increase of the pressure with the depth. In this case, the validation of the ray-tracing code is performed by comparing the result from the code with the analytical solution.

Considering that the sound velocity in an underwater application is given by the relation:

$$c(x) = c_0 + c_0 \alpha x \tag{9}$$

where c_0 is the surface sound velocity, x is the depth and α is attenuation factor, an analytical solution of the acoustic propagation can be deduced from the Snell-Descartes law:

$$\frac{sin\theta}{c} = \frac{sin\theta_0}{c_0} \qquad or \qquad sin\theta = sin\theta_0 \left(1 + \alpha x\right) \tag{10}$$

The angle θ is given in each point of the propagation curve by:

$$sin\theta = \frac{dy/dx}{\left(dy^2/dx^2 + 1\right)^{0.5}} \tag{11}$$

Combining equations 10 and 11, we obtain:

$$dy/dx = \pm \frac{sin\theta_0 \left(1 + \alpha x\right)}{\left(1 - sin^2\theta_0 \left(1 + \alpha x\right)^2\right)^{0.5}} \tag{12}$$

The integration of this equation gives the equation of the propagation curve:

$$\left(y - cot\theta_0/\alpha\right)^2 + \left(x + \frac{1}{\alpha}\right)^2 = cosec^2\theta_0/\alpha \tag{13}$$

This equation represents a circle centered in $\left(-1, cot\theta_0\right)/\alpha$ and with a radius of $cosec\theta_0/\alpha$

The acoustic propagation in an ocean, calculated analytically and via ray-tracing modeling, are presented on Fig.5. These determinations have been performed considering $\alpha = 0.05$, a surface sound speed of 1500 m/s and $\theta_0 = 45$ deg. The analytical solution is represented by the red dashed line, and the modeling is indicated by the continuous blue line. The two solutions are perfectly matching.

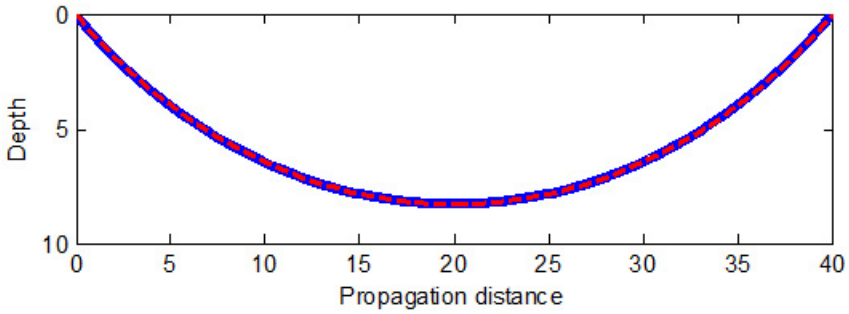

Figure 5 – Acoustic propagation in an ocean considering the variation of sound velocity due to the pressure variation from analytical development (red dashed) and from the ray-tracing modeling (continuous blue).

3.3 Application to the MYRRHA conditions

The ray-tracing modeling has been applied to the MYRRHA conditions for determining the expected influence of the velocity and temperature gradients on the propagation of ultrasonic waves. These simulations have been performed considering water as medium for matching with the experimental tests that will be performed later.

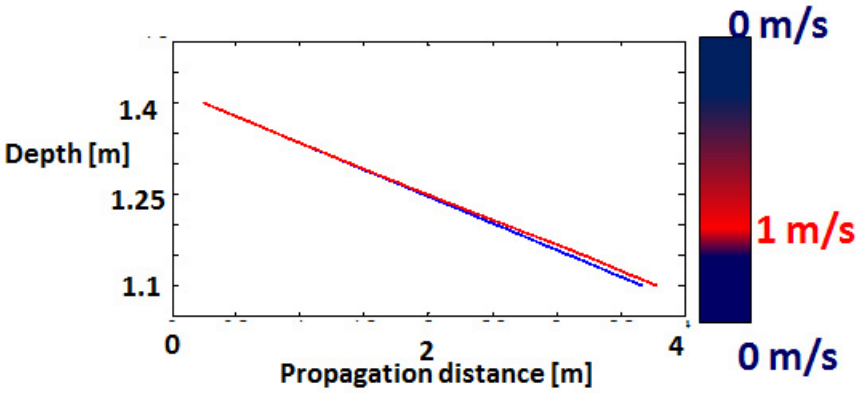

Figure 6 – Propagation of an acoustic wave emitted at 5 deg without (blue) and with velocity gradient (red).

According to the numerical simulations of the flow in the core of the MYRRHA reactor, the velocity gradient is 1 m/s over 0.2 m. This gradient has been modeled in the TAUPE facility configuration. In this configuration, the velocity gradient is horizontal and centered at 1.25 m. Out of the gradient, the velocity is considered as zero. The upper part of the gradient is a rising region where the velocity varies from 0 m/s at 1.35 m to 1 m/s at 1.175 m. Between 1.175 and 1.15 m the velocity is coming back to 0 m/s. The sensor emitting the ultrasonic wave is located at $(0.3, 1.4)$ and the emission direction is varying from 0 to 90 deg with respect to the jet axis. The propagation of an acoustic wave emitted at 5 deg is presented on Fig.6 without velocity gradient (blue) and with velocity gradient (red). The color bar on the right hand side of the figure represents the velocity. Considering the crossing between the acoustic wave and the 1.1 m depth line, the velocity gradient induces a horizontal displacement of the wave depending on the emission direction. Table 1 presents the horizontal shift of the acoustic wave for various emission angles. As we can see in this table, the effect of the velocity gradient present in the MYRRHA reactor is very low.

Table 1 – Horizontal shift of an acoustic wave due to a velocity gradient.

Angle [degree]	90	80	60	45	5	0
Shift [mm]	$\prec 0.1$	$\prec 0.1$	$\prec 0.1$	0.25	1.12	10

The temperature gradient in the core of the MYRHHA reactor is about 5 K over 0.1 m. The effect of this gradient has been determined from the ray-tracing modeling for various acoustic propagation angle and various gradient amplitude. For these simulations, the configuration considers a constant temperature

of 293 K above $x = 0$ and a linear gradient below this position followed by a second constant temperature region. The location and the temperature of this region is depending on the gradient parameters. This configuration is presented on Fig.7 for an emission angle of 5 deg and for various gradients. On this figure, a shift d is defined as the distance between the final position of the acoustic wave after a constant propagation time. The values of this shift d are presented in Table 2.

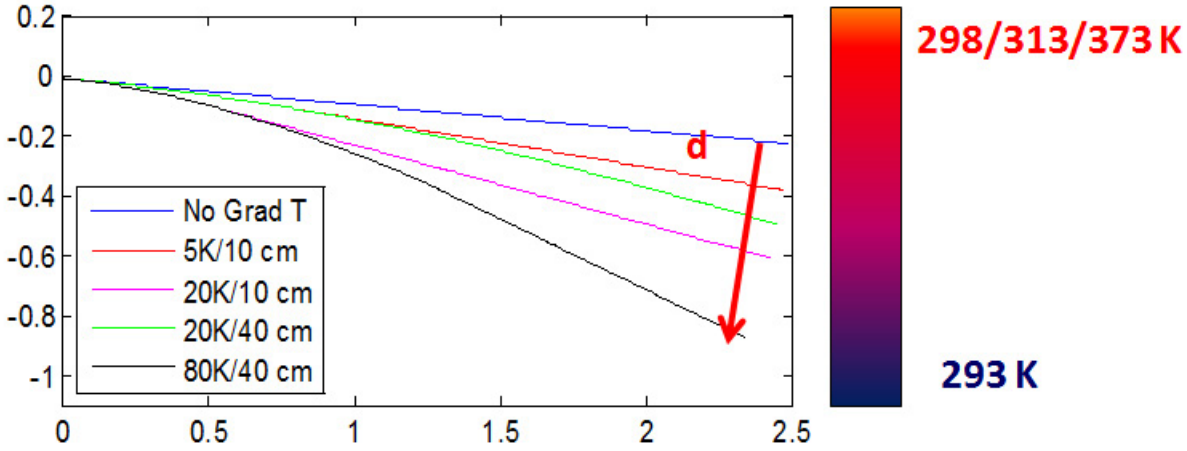

Figure 7 – Effect of temperature gradient on the propagation of an acoustic wave in water for various gradient parameters.

Table 2 – Final position shift due to temperature gradient [mm].

	75	60	45	30	5
5K/0.1m	6	13	22	38	156
20K/0.1m	21	43	73	120	387
20K/0.4m	20	41	70	113	272
80K/0.4m	58	122	201	313	667

The variation of the temperature influences also the velocity of the acoustic wave. Table 3 presents the variation of the distance traveled by an acoustic wave during a constant propagation time.

Table 3 – Variation of the traveled distance due to temperature gradient [mm].

	75	60	45	30	5
5K/0.1m	24	24	24	24	20
20K/0.1m	80	80	79	79	72
20K/0.4m	75	74	73	70	41
80K/0.4m	222	222	216	208	156

4. CONCLUSION

A new water test facility has been designed and mounted for investigating the effects of flow conditions in the core of a next generation nuclear reactor on the propagation of ultrasonic waves. These waves are used for the visualization and the inspection of the internal structure of the core of these reactors cooled with lead-bismuth liquid metal. The choice of the water as medium for test facility comes from the acoustic similarity between the lead-bismuth and the water, and the complexity and dangerousness of working with lead-bismuth. The new facility is equipped with a Shadowgraph system for the visualization of the propagation in water. This system is composed of optical accesses covering the entire height of the facility, four mirrors for creating the parallel light beams, and a high speed camera. All these elements are supported by a structure mounted on vertical displacement system for following the acoustic beam over

large distances. The design of the new facility has considered the generation in the facility of velocity and temperature gradients representatives of gradients in the core of the MYRRHA reactor.

A modeling algorithm based on the ray-tracing principle has been developed, implemented and validated. The validation is based on the comparison of the modeling results with the CFD calculation and analytical development for non-homogeneous configurations. This algorithm has been used for modeling the propagation of acoustic waves in the conditions of the MYRRHA reactor. From this, the effect of the velocity gradient on the propagation has been shown very low with a maximum shift of the acoustic beam of 10 *mm* or 75% of the ultrasonic sensor diameter. The effect of temperature gradient is clearly higher with a maximum final position shift of the acoustic wave, for constant propagation time, from 156 *mm* for a gradient of 5K over 0.1 *m* to from 667 *mm* for a gradient of 80K over 0.4 *m*. Furthermore, the variation of the temperature induces a variation of the propagation distance in a fixed propagation time. This variation reaches 222 *mm* for a gradient of 80K over 0.4 *m*.

ACKNOWLEDGMENTS

This research is performed in collaboration with the SCK-CEN and is funded through the DEMOCRITOS research contract financed by BELSPO (Belgian Science Policy Office).

REFERENCES

1. Abderrahim H, Kupschus P, Malambu E, Benoit P, VanTichelen K, Arien B, et al. MYRRHA: A multipurpose accelerator driven system for research and development. Nuclear Instruments and methods in physics research. 2001;463:487–494.

2. Carchon R, Borella A, van der Meer K. Design information as the basis for effective safeguards: the case of MYRRHA. In: 31st Esarda Annual meeting; 2009. .

3. Lyons R. Understanding digital signal processing (Third edition). Prentice Hall PTR; 2010.

4. Kazys R, Voleisis A, Sliteris R, Voleisiene B, Mazeika L, Abderrahim H. Research and development of radiation resistant ultrasonic sensors for quasi-image forming systems in a liquid lead-bismuth. ISSN 1392-2114 ULTRAGARSAS (ULTRASOUND). 2007;62:7–15.

5. Kazys R, Voleisis A, Sliteris R, Mazeika L, VanNieuwenhove R, Kupschus P, et al. High temperature ultrasonic transducers for imaging and measurements in a liquid lead-bismuth eutectic alloy. Transactions on ultrasonics, ferroelectrics and frequency control. 2005;52/4:525–537.

6. Jasiuniene E. Ultrasonic imaging techniques for non-destructive testing of nuclear reactors, cooled by liquid metals: review. ISSN 1392-2114 ULTRAGARSAS (ULTRASOUND),. 2007;62:39–43.

7. Dierckx M, Van Dyck D, Vermeeren L, Bogaerts W. Research Towards Ultrasonic Systems to Assist In-Vessel Manipulations in Liquid Metal Cooled Reactors. Nuclear Science, IEEE Transac. 2014;61/4.

8. Krautkramer F, Krautkramer H. Ultrasonic testing of material. Springer-Verlag; 1977.

9. Raman C, Nagenda N. The diffraction of light by high frequency sound waves, Part 1. Proc Indian Acad Sci. 1936;A2:406–412.

10. Bucaro J, Dardy H. Sensitivity of the schlieren method for the visualization of low-frequency ultrasonic waves. J Acoust Soc Am. 1978;63/3:768–773.

11. Neumann T, Ermert H. A new designed Shlieren system for the visualization of ultrasonic pulsed waves fields with high spatial and temporal resolution. In: IEEE Ultrasonic Symposium; 2006. .

12. Pierce AD. Acoustics, an introduction to its physical principles and applications. In: Acoustical Society of America; 1994. .

13. Candel S. Numerical solution of conservation equations arising in linear wave theory: application to aeroacoustic. J Fluid Mech. 1977;83/3:465–493.